프리스트레스트 콘크리트 박스거더 교량 부재의 정착부 균열하중 및 극한하중의 예측

Prediction of Cracking and Ultimate Loads of Prestressed Concrete Anchorage Zones in Box-Girder Bridges

임동환* 오병환**
Lim, Dong Hwan Oh, Byung Hwan

요 약

프리캐스트 프리스트레스트 콘크리트 박스거더 교량의 정착부에 프리스트레스 힘이 도입되면, 과다한 국부집중 하중으로 인하여 균열이 발생할 수 있으며, 최근 이러한 교량의 건설시 텐던을 따라가며 심각한 균열이 발생한 경우가 있다.

본 논문은 프리캐스트 프리스트레스트 콘크리트 상자형 교량의 정착부에 발생하는 국부집중응력의 분포 특성을 규명하고, 프리스트레스 정착부의 파괴거동에 가장 중요한 인자로 생각되는 텐던의 경사각, 텐던의 편심 및 콘크리트의 연단두께 등이 정착부 파괴에 미치는 효과등을 규명하고, 이들 변수를 포함하는 정착부 균열하중 및 극한하중 예측식을 제안함에 그 목적이 있다. 이를 위하여 정착부 파괴에 직접적인 영향을 미치는 단면의 형상, 텐던의 배치상태등을 변수로 하는 비선형 유한요소 해석이 수행되었다. 본 연구에서는 단면의 기하학적 형상 및 배근 방식에 따른 초기균열하중 및 극한하중 예측식이 제안되었다.

Abstract

Recently, several prestressed concrete box girder bridges have experienced severe cracking along the tendon path when prestress force has been transferred to the anchorage zone.

The purpose of the present study is therefore to explore characteristics of the local stress distribution, to study the effects of section geometry of anchorage zones, i.e., tendon inclination, tendon eccentricity and concrete cover thickness and to develop recommendations for specific design criteria for post-tensioned anchorage zones. To accomplish these objectives, a comprehensive nonlinar finite element study has been conducted. From this study, realistic formulas for cracking and ultimate load capacities are proposed. These equations reasonably well predict the cracking and ultimate loads of prestressed concrete anchorage zones.

Keywords : prestressed concrete, anchorage zone, cracking loads, ultimate loads, prestressing tendon, local stress, finite element analysis.

* 정회원, 동국대학교 토목공학과 강사, 공학박사
** 정회원, 서울대학교 토목공학과 교수

• 본 논문에 대한 토의를 1994년 12월 31일까지 학회로 보내주시면 1995년 2월호에 토의회답을 게재하겠습니다.

1. Introduction

The formation of the longitudinal tendon path crack is the most important visible bench mark in the behavior of a post-tensoned anchorage zone. From a strength standpoint, cracking always seems to occur at a load below the ultimate capacity and hence serves as a warning indicator in concrete structures.

When a concentrated load is applied through a bearing plate across the width of a finite rectangular plate, compressive and tensile stresses are set up. These two tension fields are as follows ; stresses acting along the direction of loading, and stresses acting along the loading surface parallel to it. These are generally called as bursting stress and spalling stress, respectively. In dealing with a specific post-tensioned anchorage, the load must be applied over a finite area and the compressive stress immediately under the anchor plate is called bearing stress.

Cracking and ultimate loads on the anchorage zones are closely dependent on the internal tensile stresses. It is very important to determine the distribution of tensile stresses and the maximum magnitude of these stresses. The authors have conducted a comprehensive experimental study on the anchorage zone behavior and a variety of analyses are conducted with nonlinear 3-dimemsional finite element method in the present study.

Since the cracking and ultimate loads are generally influenced by the geometric variables such as cover thickness, eccentricity and inclination of tendon on the anchorage zones, these parameters were used in this parametric study. In this study, realistic formulas for cracking and ultimate load capacities are proposed. Tendon inclination, tendon eccentricity and other influencing variables are considered in deriving the formulars. The equations are compared with test data and found to reasonably well predict the cracking and ultimate loads of prestressed concrete anchorage zones.

2. Cracking Behavior at Anchorage Zones in Prestressed Concrete Members

In spite of the many variables investigated in the experimental study, the post-tensioned anchors tend to exhibit a generally consistent behavior in sequence of failure. The cracking and ultimate loads were affected by variables such as tendon's inclination, anchorage reinforcement type, structural reinforcement contents. But the modes of failure were generally the same.

The basic stages, when there are no supplementary reinforcement, are as follows ;

(a) Initial cracking along the tendon path, beginning at a distance about the bearing plate width in front of anchor.

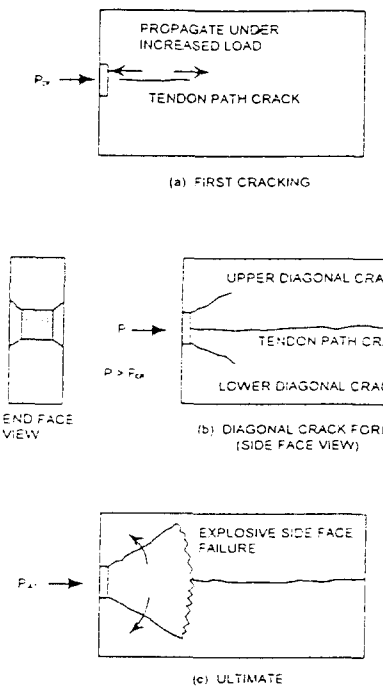

Fig.1 The modes of failure on the anchorage zones.

(b) With increased load, the crack extends both towards the loaded face and away from it.

(c) Formation of diagonal cracks on the end face, emanating from the corners of the bearing plate.

(d) Propagation of the diagonal cracks on the side faces.

(e) A generally sudden explosive-type failure, with complete destruction of the side face and a noticeable formation of a cone of crushed concrete ahead of the anchor.

These failure modes are shown in Fig.1

3. Finite Element Analysis for Anchorage Zones

The analysis with non-linear finite element method is conducted by ABAQUS supplied by Hibbitt, Karlson and Sorensen, Inc. A three dimensional isoparametric solid finite element defined by twenty nodal points having three degrees of translational degree of freedom at each node is used. To define concrete properties beyond elastic range, "CONRETE" option was used. To define the values of stress and strain at ultimate strength, "FAILURE RATIOS" option were also used.

Strain softening behavior for cracked concrete and the reduction of shear modulus associated with crack surfaces as a function of tensile strain across crack are also considered. These material input data were determined by material's test, and Young's Modulus(E) and Poisson's ratio(ν) are also determined by tests. Local anchorage steel and shear reinforcements have been included in this finite element model. These reinforced steel have been modeled by truss element.

For the case of inclined tendon members, tendon curvature are required, and by multiple strand effects, the curvature forces directed to the center of curvature are generated. These curvature forces are calculated exactly by making programs, and this calculated forces are applied to the nodal point by concentrated loads. By these modeling, moments and forces are equilibriumed at any points.

4. Parametric Study with Non-linear Finite Element Method

The concrete failure is greatly affected by the geometric variables such as tendon's eccentricity, inclination, and proportions of the section. With non-linear finite element method using ABAQUS, the geometric parameters were studied in this analysis program.

To determine geometric effects, a variety of analysis are performed, and the main variables are as follows : The eccentricity of prestress force is chosen by 0, 15, 30cm from the distance of neutral axis, and the inclination of tendon is selected by 0°, 5°, 10°, 15°, and 20°. And the concrete cover thickness of member is chosen by 20cm, 35cm, 50cm.

In this following sections, these parameter's effects are described in detail.

4.1 Inclined Tendon Effects

4.1.1 Cracking and Ultimate loads

To explore the effect of inclination tendon, curved tendon members with 0°, 5°, 10°, 15°, and 20° degree's tendon profile, were analyzed. Table 1 gives data summary of cracking load according to member's geometry.

From these results, it can be seen cracking and ultimate load are decreased as the inclination of tendon increases. As shown in this table, the cracking load of straight tendon member have 293ton, but inclined tendon mem-

bers −20 degrees− have lower cracking load about 181ton. It is thought that the geometric shape of tendon induces the radial tensile force directed to the center of curvature, and by these tendon curvature force the cracking and ultimate load reduced significantly. From this results it is shown that cautious considering are necessary when tendon are setted on high degree inclination, and the range of tendon inclination is desirable to 15 degree below.

Fig.2 shows the cracking loads compared with test data as a function of tendon inclination. As shown in this figure, there were a drop in cracking loads of 1.9% as increasing 1 degree increase of tendon inclination. This reduction values are slightly lower than test data −1.3%.

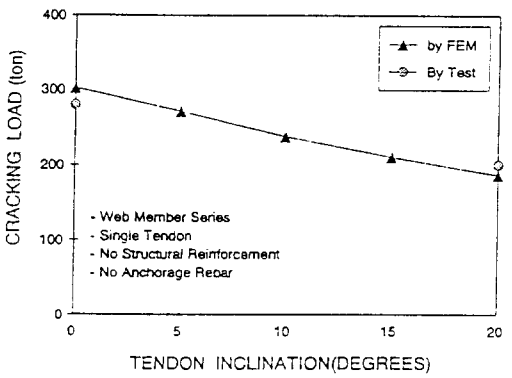

Fig.2 Cracking loads compared with test data as a function of tendon inclination.

4.1.2 Local Stress Distribution

When the inclination of tendon is varied, the characteristics of local stress distribution on anchorage zone are studied in this section. Fig. 3 shows the tangential bursting stress contours to the direction of y axis. As shown in this figure, there is the region of bursting tensile stress and spalling stress. As shown in Fig.3, bursting stress zone is shown at the front of live end, and the peak tangential bursting stress is located at the distance of 20−30cm (approximately 2a′), and this peak tangential stress may induce the first cracks. In experimental test by Lim, D.H. et al., the first cracks are shown in this position of distance from anchor plate, and these facts are well agreed the non-linear 3−D FEM results. Generally, for the case of curved tendon member, curvature tensile stress is shown at the beneath of the tendon, and this is due to prestress steel's jamming phenomenon by its geometric shape.

Table 1 Geometric properties and cracking loads

Members	Cover thickness t,(cm)	Width of anchor 2a′(cm)	Compressive stress σ_{ck}(kg/cm^2)	Width of section 2a(cm)	Eccentricity of tendon e,(cm)	Inclination of tendon θ, degrees	Cracking load P_{cr}(ton)
1	40	26.5	500	120	0	0	302
2	40	26.5	500	120	0	5	271
3	40	26.5	500	120	0	10	238
4	40	26.5	500	120	0	15	210
5	40	26.5	500	120	0	20	186
6	40	26.5	500	120	15	0	252
7	40	26.5	500	120	30	0	222
8	40	26.5	500	120	15	20	180
9	40	26.5	500	120	30	20	175
10	70	26.5	500	120	0	0	321
11	100	26.5	500	120	0	0	330
12	70	26.5	500	120	0	20	196
13	100	26.5	500	120	0	20	202

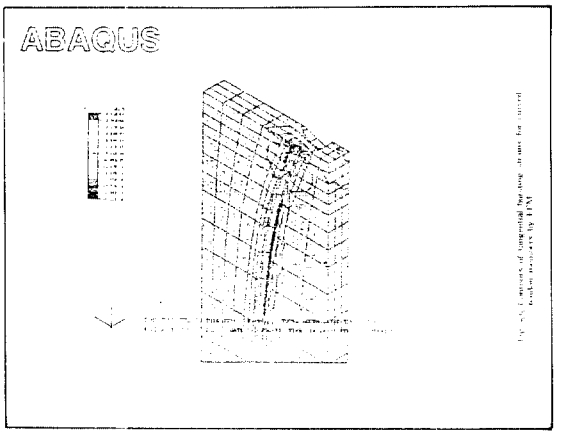

Fig.3 Tangential bursting stress contours to the direction of y axis.

Fig.4 shows the tangential bursting stresses at the upper side of tendon(at point B) according to the distance from the loaded face. As shown in this figure, peak tangential stress, when the inclination of tendon increases, are revealed lowly. For example, when prestress force is got at a force of 90 ton, the peak stress of the straight tendon member 24.69 kg/cm^2, but that of 20° inclined member are shown at the value of 20.64kg/cm^2. And radial bursting stress shows also similar characteristics. It may be thought that tendon curvature force induced the compression stress at the upper face of tendon, and this stress is compensated with tensile stress at the upper side of tendon. This stress tendency is also noticed at the test results, and is well agreed with Breen's test results.

Fig.5 shows the radial bursting stress at the side face of tendon according to the distance from the loaded face. It is shown that, as increases tendon inclination, bursting stresses are noticed highly, and for the highly inclined member, tendon curvature force is generated higher than straight tendon member. Therefore, when design precast segment bridge, the effect on the tendon inclination must be considered seriously, and as for the case of highly tendon inclination, the reinforcement of spiral steel is necessary.

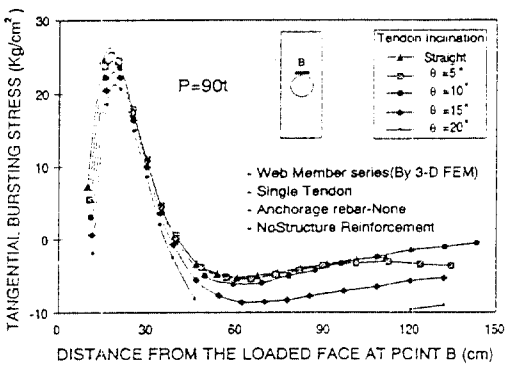

Fig.4 Tangential bursting stress distribution as a function of tendon inclination.

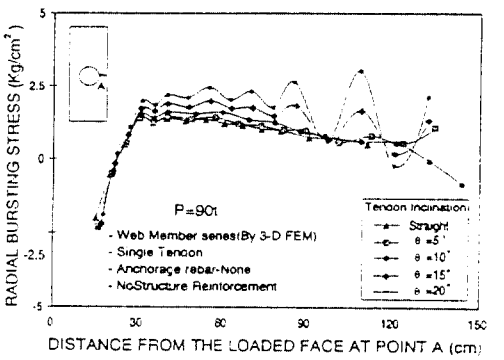

Fig.5 Radial bursting stress distribution as a function of tendon inclination.

An anchor located 1/2 of the way toward the edge will crack at a load approximately 26% below that for centroidal loading. The trend appears to be fairly linear. For the case of curved tendon(θ=20°) member, the reduction of cracking loads are shown relatively low. This is the cause of loading direction. In this FEM analysis, the size of members is restricted with test members. And the direction of eccentricity must be below the centroidal plane.

4.2 Effects of Tendon Eccentricity

4.2.1 Cracking and Ultimate Loads

To explore the effect of tendon's eccentricity, straight and curved tendon members(θ =20°) with eccentricity tendon were analyzed. And the eccentricity from neutral axis varied from e=0 to e=30cm(e=0.5a).

Fig.6 shows the cracking load as function of tendon's eccentricity. As shown in this figure, for straight tendon member, an anchor located 1/4 of the distance from the centroidal plane toward the edge will crack at a load approximately 16% below that for centroidal loading.

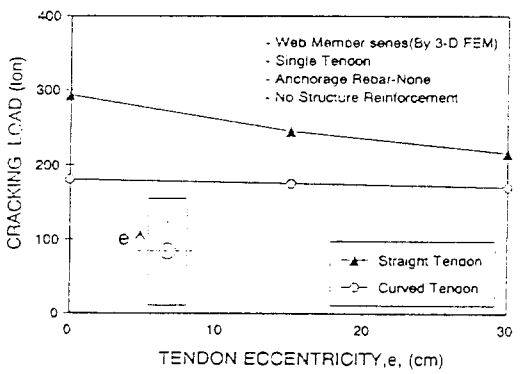

Fig. 6 Cracking load as a function of tendon eccentricity.

4.2.2 Local Stress Distribution

Fig.7 shows the comparison of the tangential and radial bursting stresses at P=90t as for the straight tendon member when increases the tendon's eccentricity. As shown in this figure, tangential bursting stress are increased significantly as increase eccentricity. Specially, the increasing ratio between eccentricity= 0cm and eccentricity=15cm is very large and this is the cause of cracking and ultimate load reduction. And radial bursting stress also increases when increases eccentricity.

Thus it is necessary to reinforce with steel when increases tendon's eccentricity.

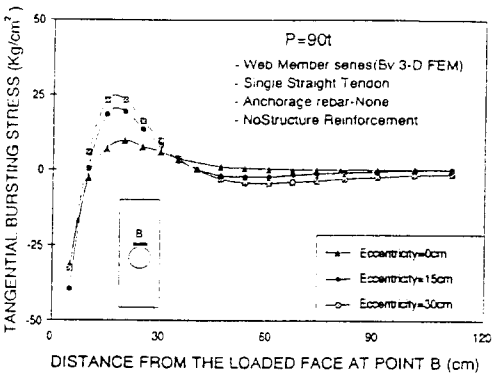

Fig.7 Tangential bursting stress distribution as a function of tendon eccentricity.

4.3 Effects of Concrete Cover Thickness

4.3.1 Cracking and Ultimate Loads

To examine the effect of concrete cover thickness, straight and curved tendon(θ=20°)members with different concrete cover thickness were analysed. And the concrete cover thickness varied from t=20cm to t=50cm. Fig.8 shows the cracking load as a function of concrete cover thickness. As shown in this figure, for the case of straight tendon series, a member with 30cm thickness cracked at a load 6.5% higher than that with 20cm thickness, and a member with 50cm thickness cracked 9% higher than that with 20cm. For the case of cur-

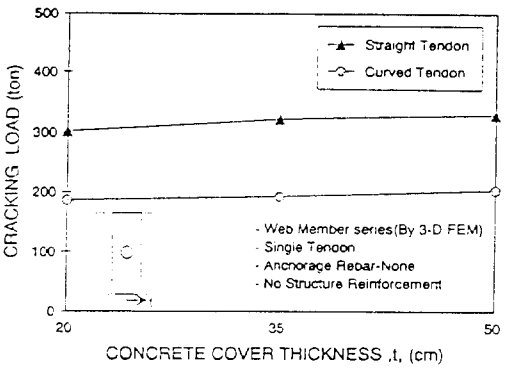

Fig.8 Cracking load as function of concrete cover thickness.

ved tendon, the increase ratio of cracking load is lower than that of straight tendon.

Although increasing ratio of the cracking load is lower as increase cover thickness, but as increase concrete cover thickness, the resistance of ultimate state is very high.

4.3.2 Local Stress Distribution

Fig.9 shows the comparison of the tangential bursting stress, as increase concrete cover thickness of straight tendon member series, when prestress force transferred at p=218t. As shown in this figure, tangential bursting stress reduced significantly reduced as increase cover thickness. This is the main cause of cracking and ultimate load's increase. It is seen that thick concrete cover can be the tools of reducing internal tensile stress.

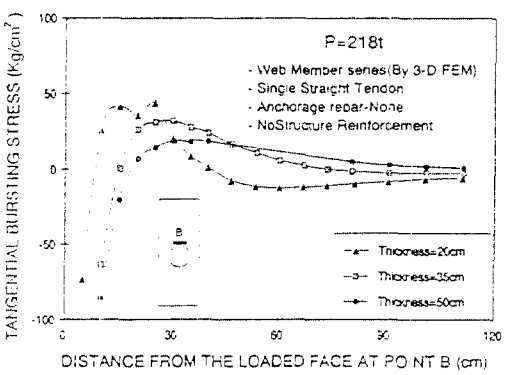

Fig.9 Tangential bursting stress distribution as a function of concrete cover thickness.

5. Development of Design Criteria

5.1 Cracking and Ultimate Load Prediction

A step-wise multiple linear regression analysis considering all geometric variables-tendon inclination, eccentricity, concrete cover thickness, anchorage width and the height of the member was performed using the results of 14 tests for which no anchorage zone reinforcement was provided. Both model and full scale test member's data was supplied by Seoul National University and Breen's test results.

Table 2 shows the regression analysis data used in this study. Using this data, a large number of variable combinations were examined. The regression analysis was performed using the program IMSL. In this manner, a large number of runs could be made efficiently, and the variables with low statistical meaning were deleted.

The primary goal of this regression study was to minimize the mean standard error which is a measure of the difference between the measured and calculated cracking loads, using a reasonable expression. The resulting general cracking load equation is expressed as a function of six major variables. The resulting expression is as follows :

$$\begin{aligned} P_{cr} = {} & 87.869f_c + 1.389(2a') - 6.305(2a) \\ & + 4.339e + 2.614\theta - 11.93t \\ & + 0.235(2at) - 229.02(e/2a) \\ & - 11.96(2a'/t)^2 - 0.3(e/2a)^2t^2 \\ & - 0.004(\theta t^2) + 309.23 \end{aligned} \quad (1)$$

Where, P_{cr} : cracking load(ton)

e : eccentricity(cm)

2a : section height(cm)

2a′ : width and depth of bearing area (cm)

t : section thickness

θ : tendon inclination(degrees)

To demonstrate the accuracy of Eq.1, comparison between the measured experimental cracking load and the calculated value is conducted. These results are shown in Table 3. As shown in this table, the mean of $P_{cr(observed)} / P_{cr(calculaetd)}$ was 1.008.

And ultimate load equation is expressed as a function of six major variables. The resulting

expression is as follows ;

$$P_{ul}=138.7f_c+2.194(2a')-6.282(2a)+24.086(e)+7.47(\theta)-11.04t+0.232(2at)-1213.348(e/2a)-7.216(2a'/t)^2-0.703(e/2a)^2t^2-0.005(\theta t^2)+280.783 \quad (2)$$

As shown in this table, the mean of $P_{cr(observed)}/P_{cr(calculaetd)}$ was 1.004. Equation 1 used to predict the plate anchor load- especially VSL type anchorage- which will cause cracking in a section without anchorage zone reinforcement. Equation 1, althougth intended for general application, has certain restrictions due to lack of data in certain areas. These include ;

(1) Multiple tendons anchored in the same section are not covered.

(2) The anchorage is assumed to be square section.

Table 2 Data for regression analysis

Members	Cover thickness t,(cm)	Width of anchor 2a'(cm)	Compressive strength σ_{ck}(kg/cm^2)	Width of section 2a(cm)	Eccentricity of tendon e,(cm)	Inclination of tendon θ, degrees	Cracking load P_{cr}(ton)	Ultimate load P_{ul}(ton)
MR1A	7.62	6.67	393	52.07	0	0	17.69	29.45
MR1B	7.62	5.40	394	52.07	0	0	19.50	24.04
MI1B	7.62	5.40	375	52.07	0	0	18.60	22.68
M7C4	7.62	5.08	277	50.8	7.62	0	14.52	16.33
FS1A	30.48	21.59	352	208.30	0	0	181.44	204.12
FS2B	30.48	26.67	324	208.00	0	30	149.69	281.23
M1A4	7.62	5.08	251	50.80	15.24	0	8.16	8.16
FS1B	30.48	26.67	405	208.00	0	0	181.44	208.66
M1-2	10.16	5.08	298	50.80	50.8	0	19.50	19.50
M2-2	7.62	5.08	298	50.8	0	0	15.42	15.42
M3-2	5.08	5.08	298	50.8	0	0	10.89	10.89
M2A-4	11.43	5.08	251	50.8	15.24	0	9.98	9.98
W-SS-A0-R0	40.00	26.50	500	120	0	0	280.00	–
W-SC-A0-R0	40.00	26.50	500	120	0	20	205.00	320.00

Table 3 Comparison of theory with experimental data for cracking loads

Members	Cracking Load(Pcr)			Ultimate Load(Pu)		
	$P_{cr,observed}$	$P_{cr,calculated}$	$P_{cr,ob}/P_{cr,cal}$	$P_{ul,observed}$	$P_{ul,calculated}$	$P_{ul,ob}/P_{ul,cal}$
MR1A	17.69	17.91	0.998	24.95	25.03	0.997
MR1B	19.50	19.38	1.006	24.04	24.27	0.991
MI1B	18.60	17.71	1.050	22.68	21.63	1.049
M7C4	14.52	13.44	1.080	16.33	14.22	1.148
FS1A	181.44	179.19	1.013	204.12	201.18	1.015
FS2B	149.69	147.53	1.015	281.23	291.23	0.966
M1A4	8.16	8.65	0.943	8.16	9.35	0.873
FS1B	181.44	187.70	0.967	208.66	217.67	0.959
M1-2	19.50	19.24	1.014	19.50	19.71	0.989
M2-2	15.42	16.91	0.912	15.52	16.41	0.940
M3-2	10.89	10.25	1.062	10.89	10.51	1.036
M2A-4	9.98	9.66	1.033	9.98	9.38	1.064
W-SS-A0-R0	280.00	178.85	1.004			
W-SC-A0-R0	205.00	203.13	1.009	320.00	312.45	1.024

5.2 Effects of Anchorage Local Reinforcement and Other Variables

Cracking loads calculated from Eq.1 represents the expected value for normally reinforced section without anchorage zone reinforcement. A substantial member of this tests dealing with anchorage reinforcing methods-orthogonal tie type reinforced and spiral reinforced-indicated that cracking loads could be raised by addition of such reinforcement.

Assuming linear variation between the values for the reinforced ratio of local reinforced steel and stirrups, the cracking load of the members that reinforced by local anchorage steels are as follows ;

$$P'_{cr}=P_{cr}(1.08\ \rho_{spiral}+1.62\ \rho_{stirrup})+14.89 \quad (3)$$

Comparison between the measured experimental cracking load and the calculated value for the members reinforced with local and shear steel is conducted. These results are showen in Table 4. As shown in this table, the mean of $P_{cr(observed)}/P_{cr(calculated)}$ was 1.001 with a standard deviation.

Table 4 Comparison between the measured experimental cracking load and the calculated value for the members reinforced with local and shear steel

Members	Cracking load(ton)		$P_{cr,ob}/P_{cr,cal}$
	$P_{cr(observed)}$	$P_{cr(calculated)}$	
FS3A	167.83	166.34	1.009
FS4A	181.44	185.67	0.977
W-SS-A2-R0	296.00	297.34	0.996
W-SC-A2-R0	220.00	220.55	0.998
W-SS-A2-R1	300.00	299.30	1.002
W-SC-A2-R1	226.00	221.2	1.022

5.3 Comparisons of Experimental Results with Various Design Codes

1) ACI and PTI

ACI and PTI's design provisions are based on an allowable bearing stress equation presented in ACI Commentary and Post-Tensioning manual. The permissible bearing stress after allowance for stress losses is as follows.

$$f_b=0.6\ f_{ci}\sqrt{A_2/A_1} < f_{ci} \quad (4)$$

Comparison of ACI code with test results is rather difficult because ACI code gives only the specification of permissable bearing stresses. To compare the experimental ultimate load with ACI design code, bearing force P_b by ACI design code was computed by multipling the allowable bearing stress by the gross area of the anchor plate. A comparison of the bearing force P_b calculated by ACI design code with observed ultimate loads from experimental tests is listed in Table 5.

The ACI-PTI's equation were conservative about 15% for all the test members. But this equation is restricted to straight tendon and can not be applied to the other geometry such as curved tendons.

Table 5 Comparisons of observed ultimate load with ACI code

Members	Observed Ultimate Load $P_{ul,obs}$(ton)	Calculated Bearing Force by ACI, $P_{b,cal}$(ton)
W-SS-A0-R1	-	293
W-SS-A1-R1	336	293
W-SS-A0-R2	344	293
W-SS-A2-R0	328	293
W-SS-A2-R1	340	293

2) CEB-FIP

The Comite' Euro-International du Beton (CEB) and the Federation International de la Precontrainte(FIP) prescribe that for the case of uniform distributed pressures, the local resisting force shall be determined as follows,

$$f_{cc}^{*}=0.67\, f_{cc}\sqrt{A_2/A_1} \le 4\, f_{cc} \qquad (5)$$

Therefore, both ACI and CEB-FIP codes have the same type of formular for admissable bearing stresses. The CEB bearing stresses are substantially higher, because of the safety factor of concrete.

Comparison of CEB-FIP code with test results is also difficult, because CEB-FIP code gives only the specification of permissable bearing stresses. To compare the experimental ultimate load with CEB-FIP design code, bearing force P_b was computed by multipling the allowable bearing stress by the gross area of the anchor plate. A comparison of the bearing force P_b caculated by CEB-FIP design code with observed ultimate loads from experimental tests is listed in Table 6. The CEB-FIP equation were conservatively coincided with test results. But this equation is restricted to straight tendon and can not be applied to the other geometry such as curved tendons.

Table 6 Comparisons of observed ultimate load with CEB-FIP code

Members	Observed Ultimate Load $P_{cr,obs}$(ton)	Calculated Bearing Force by CEB FIP, $P_{b,cal}$(ton)
W-SS-A0-R1	–	328
W-SS-A1-R1	336	328
W-SS-A0-R2	344	328
W-SS-A2-R0	328	328
W-SS-A2-R1	340	328

3) Stone and Breen

Stone and Breen's design equation calculates the cracking load P_{cr} considering tendon's inclination and eccentricity as follows ;

$$P_{CRplate}=t[f_{sp}(38a-120) - \frac{t}{81}(20-252(e/a)f_{sp}) - \frac{103}{9}(e/a)-7]+39a' + \frac{f_{sp}}{5}[166-975(a'/t^2)]-9.1 \qquad (6)$$

Stone and Breen found that the presence of supplemental reinforcement did increase the cracking load and they accounted for this expected rise by modifying the results of above equation as follows :

$P_{cr}=(2.03-0.032\theta)$

P_{cr} : spiral reinforcement

$P_{cr}=(1.61-0.019\theta)$

P_{cr} : orthogonal reinforcement (7)

Table 7 shows the comparison of observed and predicted cracking load caculated by Stone and Breen and this study. As seen in this table, Stone and Breen's predicted equaton were conservative for most of members except for spiral anchorage reinforced members. Table 7 also indicates that the deviation of the Stone & Breen formular from test data is very large, especially for members without local anchorage reinforcements. But predicted equation by this study is accurately accorded with test results. Fig. 10 shows the comparison of cracking load caculated by Stone and Breen

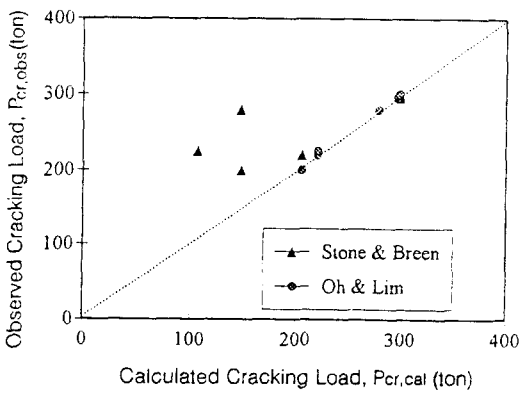

Fig.10 A comparison with the cracking load caculated by Stone & Breen

Members	Cracking load(ton)			$P_{cr,th}/P_{cr,cal}$ by Stone & Breen	$P_{cr,ob}/P_{cr,cal}$ by this study
	$P_{cr,observed}$ by test	$P_{cr,calculated}$ by Stone & Breen	$P_{cr,calculated}$ by this study		
WSC-A0-R0	200	148	205	1.35	0.98
WSS-A0-R0	280	148	279	1.89	1.00
WSS-A2-R0	296	300	297	0.99	0.99
WSC-A2-R0	220	206	221	1.07	0.99
WSS-A2-R1	300	300	299	1.00	1.00
WSC-A2-R1	226	207	221	1.10	1.02

and this study.

6. Conclusions

The purpose of the present study is to explore characteristics of the local stress distributions, and to suggest realistic formulas for cracking and ultimate load capacities of prestressed anchorage zones. To accomplish these objectives, a comprehensive analytical study has been conducted. Major variables include tendon inclination, tendon eccentricity and concrete cover thickness.

From this study, the following conclusions can be drawn.

1. Section geometry such as tendon inclination, tendon eccentricity and concrete cover thickness affects the cracking and ultimate loads. As tendon inclination increases, the cracking load capacity decreases. It is also found that eccentric loading causes the reduction of cracking loads. The amount of such reduction is quantitatively determined in the present study.
2. The ratio of web thickness to section depth(t /2a) affects greatly the cracking and ultimate loads. The cracking load for the ratio of web thickness to section depth equal to 7 /12 is to higher by 6.5 percent than that for 1 /3, and it increases up to 9 percent when t /2a becomes 5 /6.
3. Realistic formulas for cracking and ultimate load capacities are proposed. Tendon inclination, tendon eccentricity and other influencing variables are considered in deriving the formular. The equations reasonably well predict the cracking and ultimate loads of prestressed concrete anchorage zones. The proposed formula may be efficiently used for design and analysis of tendon anchorage zones including straight and curved tendons.

Acknowledgement

This paper was supported by Non Directed Research Fund, Korea Research Foundation, 1993.

REFERENCES

1. Breen, J. E., Cooper, R. L., and Gallaway, T. M., "Minimising Construction Problems in Segmentally Precast Box Girder Bridges," Research Report 121-6F, Center for Highway Research, The University of Texas at Austin, August 1975.
2. Guyon, Y., Prestressed Concrete, John Willy and Sons Inc., New York, 1953.
3. Stone, W. C., and Breen, J. E., "Analysis of Post-Tensioned Girder Anchorage Zones," Research Report 208-1, Center for Transportation Research, The University of Texas at Austin, August 1980.
4. ACI Committe 318, "Building Code Requirements for Reinforced Concrete and Commentary (ACI 318-89)", American Concrete Institute, 1989.
5. American Association of State Highway and Transfortation Officials, Standard Specifications for Highway Bridges, 12th Edition, 1977.
6. Post-Tensioning Institute, PTI Post-Tensioning Manual, Illinois, 1976.
7. CEB-FIP, "Model Code for Concrete Structures", English Translation, 1990.

8. Nilson, Arther H., "Design of Prestressed Concrete," John Wiley & Sons, 1978.
9. Nawy, E. G., "Design of Prestressed Concrete," John Wiley & Sons, 1989.
10. Guyon, Y., "The Limit State Design of Prestressed Concrete," John Wiley & Sons, 1974.
11. Douglas, D. J., and Trahair, N. S., "An Examination of the Stresses in the Anchorage of a Post-Tensioned Prestressed Beams," Magazine of Concrete Research, Vol.12, No.34, March 1960, pp.9-18.
12. Iyenger, K. T. S. R., "Two-Dimensional Theories of Anchorage Zone Stresses in Post-Tensioned Prestressed Beams," Journal of the American Concrete Institute, Vol.59, No.10, October 1962, pp.1443-1446.
13. Yettram, A. L., and Robbins, K., "Anchorage Zone Stresses in Post-Tensioned Uniform Members with Eccentric and Multiple Anchorage," Magazine of Concrete Research, Vol.22, No.73, December 1970, pp.209-218.
14. Christodoulides, S. P., "Three-Dimensional Investigation of the Stresses in the End Anchorage Blocks of a Prestress in the End Anchorage Blocks of a Prestress Concrete Gantry Beam," The Structral Engineer, Vol.35 ,No.9, September 1957.
15. Leonhardt, F., "Prestressed Concrete - Design and Construction," Berlin Wilhelm & Sons, 1964.
16. Zielinski, T., and Rowe, R. E., "The Stress Distribution Associated with Groups of Anchorages in Post-Tensioned Concrete Members," Cement and Concrete Association, Research Report No.13, London, October 1962; No.9, London, September, 1960.
17. Zielinski, T., and Rowe, R. E., "Investigation of the Stress Distribution in the Anchorage Zones of Post-Tensioned Concrete Members," Cement and Concrete Association, London, Research Report No.9, September, 1960.
18. Stone, W. C., and Breen, J. E., "Anaiysis of Post-tensioned Girder Anchorage Zones," Research Report 208-1, Center for Transportation Research, The University of Texas, Austin, April 1981.
19. Stone, W. C., Paes-Filho, W. and Breen, J. E., "Behavior of Post-tensioned Girder Anchaorage Zones," Research Report 208-2, Center for Transportation Research, The University of Texas, Austin, April 1981.
20. Lim,D.H., "Anchorage Zone Behavior and Analysis of Precast Prestressed Concrete Box -Girder Bridges," Ph.D Thesis, Seoul National University, March 1994.
21. Oh,B.H., and D.H.Lim, "Local Anchorage Stresses in Prestressed Concrete Box-Girder Bridges," EASEC-4, Vol.1, pp.1079-1084, Sep. 1993.

(접수일자 : 1994. 8. 10)